Bantu AKM, et al., J Nanotechnol Nanomed Nanobiotechnol 2019, 6: 024
DOI: 10.24966/NTMB-2044/100024

HSOA Journal of
Nanotechnology: Nanomedicine & Nanobiotechnology

Research Article

# Structural and Optical Properties of Multilayered Cobalt/M (with M= Platinum or Rhodium) Thin Films Nanowires Electrodeposited into Ion Track-Etched Polycarbonate Membranes

**Kazadi Mukenga Bantu A[1,3]*, Saleh K[2,3] and Maaza M[2,3]**

[1]*Department of Physics (Materials and Nanoscience Group), University of Kinshasa, Kinshasa, Democratic Republic of Congo*

[2]*UNESCO-UNISA Africa Chair in Nanosciences-Nanotechnology, College of Graduate Studies, University of South Africa, Pretoria, South Africa*

[3]*Nanosciences African Network (NANOAFNET), National Research Foundation-iThemba LABS, Western Cape, South Africa*

## Abstract

A series of multilayered cobalt/M (M= platinum, rhodium) thin films nanowires with diameter Dp=400 nm were synthesized into ion track-etched polycarbonate membranes by electrodeposition. Scanning Electron Microscopy (SEM) displays cylindrical wires with smooth and homogeneous contours. X-Ray Diffraction (XRD) results revealed that all samples had a mixture of Hexagonal Close-Packed (HCP) and Face Centered Cubic (FCC) phases. The wires exhibit magnetic anisotropy, which is observed and is ascribed to shape anisotropy. The magnetization reversal strongly depends on the variation of the thickness between cobalt and M (M=Pt, Rh) layers. Absolute reflectance spectra of multilayered cobalt/M (M=platinum, rhodium) thin films nanowires were acquired over the range 800-2500 nm using a Cary 5000 UV-Visible-Near Infra Red Spectrophotometer. The optical specular reflectance spectrum shows a band which probably originates from a surface plasmon resonance. Therefore, the change of the thickness (wires length) was seen to control the properties of the multilayered thin films nanowires and hence their properties could be modified for desired purpose.

**PACS:** 75.70.-i Magnetic thin films and multilayers - 81.15.Pq Electrodeposition, Reflectance, nanowires.

***Corresponding author:** A Kazadi Mukenga Bantu, Department of Physics (Materials and Nanoscience Group), University of Kinshasa, Kinshasa, Democratic Republic of Congo, Tel : +24 3811441644; +24 3819206439; E-mail: albert.kazadi@unikin.ac.cd; fakazadi@gmail.com

**Citation:** Bantu AKM, Saleh K, Maaza M (2019) Structural and Optical Properties of Multilayered Cobalt/M (with M= Platinum or Rhodium) Thin Films Nanowires Electrodeposited into Ion Track-Etched Polycarbonate Membranes. J Nanotechnol Nanomed Nanobiotechnol 6: 024.

**Received:** September 17, 2019; **Accepted:** September 25, 2019; **Published:** October 02, 2019



## Introduction

Since the oscillating interchange interaction has been found in multilayered magnetics materials, the interlayers coupling in transition metals thin films (Co, Fe, Ni) separated by non magnetics elements (Pt, Cu, Ag, Au etc) is of great interest [1,2]. Multilayers nanomaterials are of considerable industrial interest because of their specific properties and many promising areas of applications in electronics or optics like X-ray and UV mirrors, giant magnetic resistance and magnetic recording, etc. [3]. One-dimensional nanomaterials such as nanorods, Nanowires (NWs) etc… have been attracting much attention due to their important role in almost all areas of nanoscience and nanotechnology [4]. Particularly, metallic nanowires are considered to be promising candidates for future electronic, sensing, and magnetic and optoelectronic applications. The performance of nanowires depends strongly on parameters like composition, shape, size, structure and also spatial distribution which are predetermined by the fabrication method and conditions. Cobalt is an important ferromagnetic material with large coercivity and high Curie temperature (≈1388 K) and is widely used in presently available magnets and magnetic recording media. In the past decade, Co nanowires have attracted intensive research interest stimulated by their diverse application in ultra high density information storage media [5]. Additionally, some novel applications like field emission devices have been explored and reported in recent years [6,7]. To produce Co/M NWs, several fabrication methods have been developed, including template-assisted assembly [8], lithography [4], magnetic field-induced self-assembly [9] and use of diblock copolymers [10,11]. Using polymer membrane filters, ferromagnetic metal nanowires have been synthesized so far. Whitney et al. reported that the arrays of Ni and Co nanowires were electrodeposited in polymer templates with the nanometer-sized pores prepared by nuclear track etching technique [12]. They found that the preferred magnetization direction is perpendicular to the film plane and enhanced coercive force as high as 680 Oe. Piraux et al. reported that the array of Co/Cu multilayered nanowires with GMR response was electrodeposited in nanoporous polymer template [13]. Blondel et al. also reported that Co/Cu and Ni-Fe/Cu multilayered nanowires with GMR response was demonstrated [14]. They synthesized the multilayered nanowires with length of 6 μm, diameter of 80 nm and each layer thickness of 5~10 nm into the nanopores of ion track-etched polycarbonate membrane filters. As demonstrated by numerous works [14,15] the fabrication of metallic nanowires in ion track-etched templates by electrochemical deposition possesses several unique advantages such as the control over size and crystallinity. In this contribution, Co nanowires were electrochemically grown in ion track-etched polycarbonate membranes and their morphology, composition, microstructure and magnetic properties of the wires

were studied [16]. Additionally, for the first time, the optical properties in the UV-vis-NIR spectral range of well aligned multilayered Co/M (M=Pt, Rh) thin films nanowires, being embedded in an ion-track template, are investigated. This paper explores the properties of multilayered thin films NWs electrodeposited in ion track-etched polycarbonate membranes in terms of reflection across the solar spectrum.

## Materials and Methods

The electrodeposition has been carried out in a conventional three electrodes Pyrex cell (50 mL) under an AUTOLAB PGSTAT (model 302N) control at room temperature. All potentials of the working electrode were measured with respect to a Saturated Calomel Electrode (SCE) reference (Ag/AgCl) and the Counter Electrode (CE) was platinum as presented in the figure 1 where we could distinguish the autolab (a), and the electrochemical cell (b) (with its three electrodes, WE, CE and RE) used for this work.

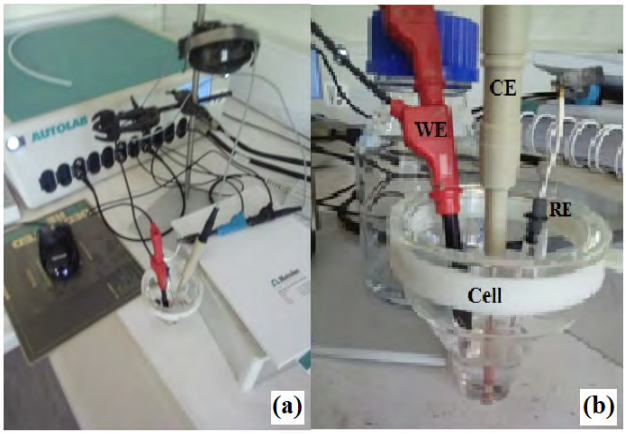


**Figure 1:** (a) Autolab PGSTAT, and (b) Electrochemical Cell with the three electrodes.

Polycarbonate (PC) membranes (from Millipore) of thickness δ≈7 µm and pores diameter ranging from 100 to 400 nm were used to produce multilayered Co/M (M=Pt, Rh) thin films nanowires. A gold (Au) seed layer was first evaporated on the backside of the PC porous membrane to cover the pores. And this backing layer served as cathode (working electrode WE) during the subsequent electrochemical deposition of the multilayered Co/M thin films nanowires. During the deposition, a negative constant voltage was applied for Co and M reduction respectively and the electric current was monitored as a function of time. The multilayered Co/M thin films nanowires were prepared alternating elemental target into PC template. The substrates dimension was ($25\pi x7x10^{-3}$) $mm^3$. The figure 2 shows the schematic transversal view of the PC membrane where δ is the thickness of the alternating deposited element Co or M.

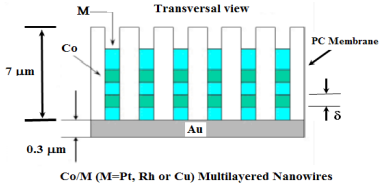


**Figure 2:** Schematic representation of transversal cross section of PC membrane showing the geometry of multilayered NWs thin films.

The electrolyte used in this work consisted of an aqueous solution as shown in the following table N° 1. To avoid the element M in the cobalt layer during the electrodeposition, we took the concentration of cobalt 100 times the concentration of the element M.

| Catalysts | BET Surface Area ($m^2/g$) | Pore Volume ($cm^3/g$) |
|---|---|---|
| $CoSO_4 \cdot 7H_2O$ (99,9%) | 1 | 100 |
| $M=K_2PtCl_6$ or $RhCl_3$ (99,8 %) | 0.01 | 1 |
| $H_3BO_4$ (99,5 %) | 40 | |

**Table N° 1:** Electrolyte composition used in this work.

The morphology of the thin films wires were studied by means of Scanning Electron Microscopy (SEM). For this last purpose, the PC membrane template was dissolved in ones drops of dichloromethane ($CH_2Cl_2$).

In addition, the microstructure and optical properties of the wire arrays were investigated by X-Ray Diffraction (XRD), the optical reflectance of the as-prepared multilayered Co/M thin films nanowires has been characterized using UV-Visible-Near Infrared Spectrophotometer (Agilent Technologies Cary Series 5000 UV-Vis-NIR Spectrophotometer) equipped with an integrating device. Reflectance spectra of the samples were measured at Room Temperature (RT) between 800nm and 2500nm. All measurements were performed in double beam mode, using reduced slit height and zero/baseline correction. Prior to the measurements, each sample was positioned using the sample clip while baseline correction was performed before the acquisition of sample spectra in order to set 0 and 100% Transmission (T) values. This is particularly important when measuring samples with low reflectance.

## Results and Discussion

### Electrodeposition processus

In order to choose the appropriate deposition potentials, the electrolyte was characterized by the Cyclic Voltammogram (CV). Figure 3 shows the stabilized cyclic voltammograms obtained for the electrolyte used to deposit cobalt/M thin films nanowires.

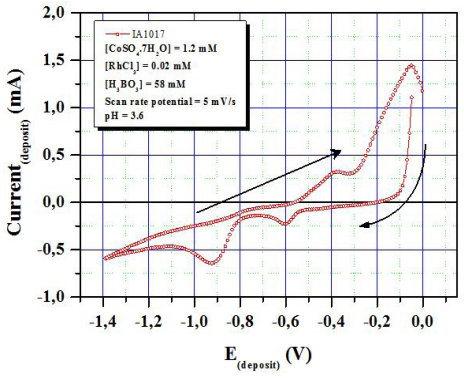


**Figure 3:** Cyclic voltammogram of the electrolyte used to deposit cobalt thin films NWs (Arrows show the scan direction).

The curve show the cathodic and anodic peaks associated to the deposition and dissolution of cobalt, respectively. There is no considerable current flowing in the potential region between 0.0 V and

-1.4 V. Cobalt depositions begin at around -0.9 V. As the absolute value of cathode potential increases from -0.80 V to -1.2 V, the current also increases. Between -1.2 V and -1.4 V, the increase of current slows down. After -1.4 V, it begins to increase with the increase of the potential. When the scan is reversed, the nucleation loop is observed. At around -0.05 V an oxidation peak of cobalt is detected. According to these results and the appearance of the films, the optimum electrodeposition potential range was decided to be from -0.80 V to -1.20V. The selected potential value is $E_d$ (Co)≈-0.90V. The same was done for M deposition potential which was decided to be $E_d$ (M)≈- 0.65V. Multilayered Co/M thin films NWs were synthesized alternatingly switching cathode potential from -0.65 V (for M layer) to -0.90 V (for Co layer) as shown in figure 4. The current-time transients were also recorded to understand the nucleation and growth mechanism of Co/M thin films nanowires. Figure 4 shows the (a) potential-time curve and (b), (c) and (d) current-time transients of the thin films nanowires.

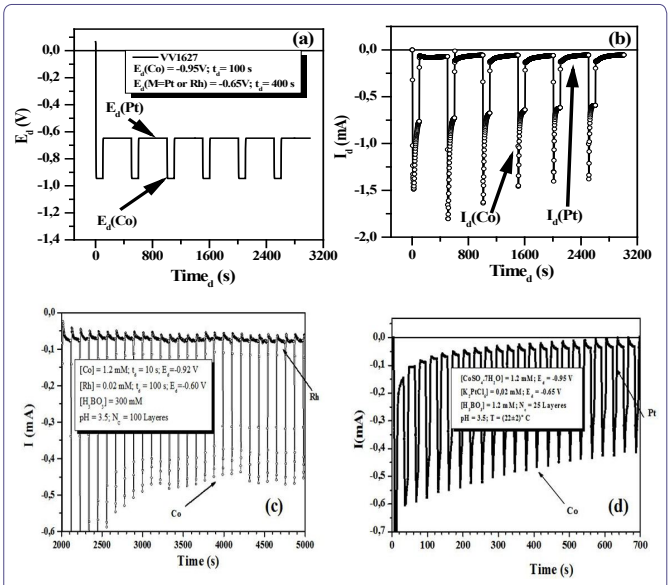


**Figure 4:** Growing process of multilayered Co/M thin films nanowires synthesized alternatingly switching cathode potential from -0.65 V (for M layer) to -0.90 V (for Co layer). (a) Potential vs time and (b) Current vs time of the thin films nanowires, (c) Cobalt/Rhodium for the 5000 first second and (d) cobalt/Platinum for the 700 first second thin films NWs.

According to this figure, when the potential is switched from -0.90 V to -0.65 V, anodic current is observed for Co/Pt. This is resulting from the dissolution of electrodeposited Co, because -0.65V is nobler than the equilibrium potential of Co. At this potential, it is estimated that the Pt deposition and Co dissolution will proceed simultaneously. According to the time - dependence of cathodic current during electrodeposition of Co/Pt multilayered nanowires as shown in figure 4(d), filling time was around 10000 s and the deposition rate was estimated to be about ≈0.7 nm/s.

## XRD characterization

The phase structure and crystalline orientation of the as-prepared multilayered Co/M thin films NWs were investigated by XRD. Figures 5(a and b) represents the XRD patterns of as prepared multilayered Co/M thin films NWs. From this analysis, it is found that the prepared particles show Hexagonal Closed Packed (HCP) crystal structure with lattice reflections of (10.0), (00.2), (10.1) and (11.0). However the relative intensity of the signal at 2θ=47.942° for Co/Pt, corresponding to the (10.1) plane, is significantly larger than for Co powder, evidencing a preferred crystallographic orientation along the (10.1) direction. [17] Predicting that nanowires of fcc materials (Co, Pt, Rh,) which are deposited potentiostatically grow preferentially along the (10.1) direction because of surface energy minimization. However, cobalt exists in two different phases-Hexagonal Closed Packed (HCP) and face centered cubic-where the fcc phase is a high temperature phase and therefore is metastable at RT. At RT this phase can also be obtained in some specific ways [7,18-20]. For electrochemically deposited Co, it has been reported that fcc structured films and nanowires were successfully fabricated with electrolytes having low pH values [7,16]. A. Kazadi et al. [3,20,21] proposed that the fcc formation is promoted by co-deposition of atomic hydrogen. In the present work, the Cobalt electrolyte consisted of 40 g/*l* $H_3BO_3$ providing a certain number of hydrogen ions which may be co-deposited during the electrochemical wire growth. According to the aforementioned mechanism, this co-deposition may promote the formation of fcc wires. Beside, Hexagonal Close Packed (HCP) (10.0), (00.2), (10.1) and (11. 0) peaks were observed at all patterns. However, in a study [20] hcp at high pH (~5.7) and fcc at low pH (~1.6) structures were observed in electrodeposited cobalt.

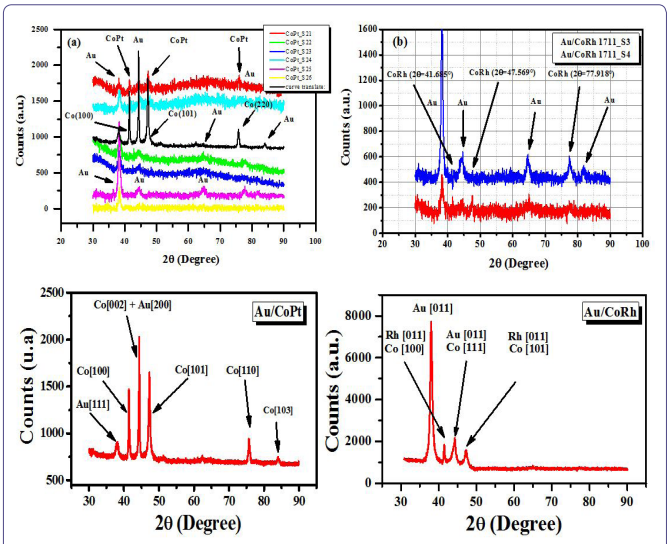


**Figure 5:** XRD patterns of multilayered Co/M thin films NWs a) M=Pt and b) M=Rh. Au (hkl): Substrate peaks. CoPt (hcp): (10.0), (00.2), (10.1) and CoRh (hcp): (10.0), (00.2), (10.1) and (10.2) peaks.

In figure 6, we could observe that the wires thickness has linear relationship with respect to the synthesis time. This indicates that there is indeed a linear relationship between the length of the nanowires and the above-mentioned time for each deposition potential.

## SEM and AFM characterization

As shown in the table N° 2, we could see the PC membrane parameters used in this work.

The SEM micrograph shown in figure 7(a) displays the morphology and size of PC template before deposition of the Co/M nanowires. And the figure 7(b) shows the top surface of PC template with hemispherical caps formed after deposition. The wires are aggregated

and randomly distributed on the substrate. The wire aggregation is ascribed to surface tension effects of solvent droplets when drying the sample after template dissolution. The detailed description of this phenomenon can be found elsewhere [22]. The SEM image presented in figure 9 and the AFM image in figure 8(a) reveal that the wires have excellent cylindrical smooth shape (highly polished surfaces), uniform deposit and homogeneous contours along their long axis. From figure 8(b), the MFM image shows the magnetic configuration of as-grown thin films, observed by magnetic force microscopy. One could notes that the magnetization is perpendicular to the wires axis in conformity to the result found for the Co wires. The polarity alternation suggests the reversal of magnetization in the perpendicular plane in function of wires' length.

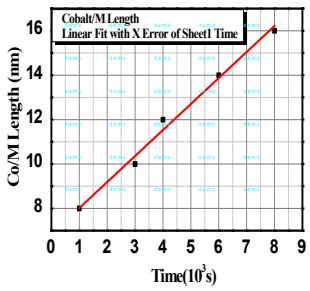


**Figure 6:** Linear relationship between the synthesis time and the thickness of wires in the polycarbonate membrane ($D_p$≈400 nm).

| Parameter | Value |
|---|---|
| Pore diameter [nm] | ≈ 400 |
| Membrane thickness [µm] | ≈ 7 |
| Pore density [pores/cm²] | ≈ 2x10$_6$ |

**Table N° 2:** Specification of PC membrane used in all experiments.

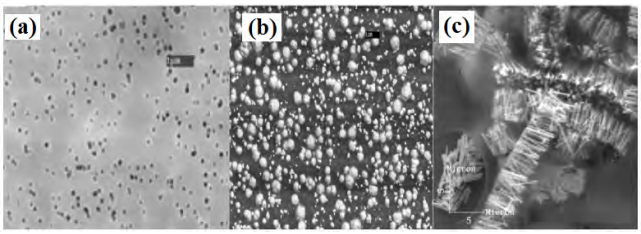


**Figure 7:** SEM images of top surface (a) before deposition and (b) after deposition with hemispherical caps formed and (c) CoM NWs after removal a part of ion track-etched PC template.

## Optical characterization

The total reflectance spectra of all the samples (Figure 9) clearly indicate the influence of layers number and electrolyte type on the interference pattern. The occurrence of interference fringes obtained for each sample is due to partial reflection on the top surface (PC template-air interface) and on the bottom surface (PC template - Au interface). For a determined wavelength, if the reflected rays on the both surfaces are in phase, they interfere constructively and originate a maximum of the reflectance spectrum. If they have opposite phases, a destructive interference occurs. And this causes a minimum on the reflectance spectrum. The number of interference maxima and minima is directly related to the multilayered Co/M thin films NWs layer thickness. Figure 9 shows the specular reflectance spectra of ($D_p$=400nm) the as-prepared multilayered Co/M thin films NWs being embedded in the PC template were measured with UV light propagating obliquely with 30° along the wires' long axis in a standard transmission mode. From the optical spectra, in the optical response, the multilayered Co/M thin films NWs show a broad reflectance band from ≈900nm to ≈2500nm which is ascribed to the so-called ''surface plasmon resonance" (SPR) [23], the collective oscillation of conduction electrons within the wires driven by the electric field of the incident light.

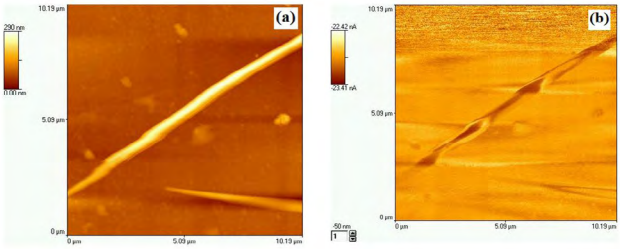


**Figure 8:** (a) Atomic Force Microscopy (AFM) and (b) Magnetic Force Microscopy (MFM) images of multi-layered CoPt thin films NWs after membranes dissolution into Tri-chloromethane ($CHCl_3$).

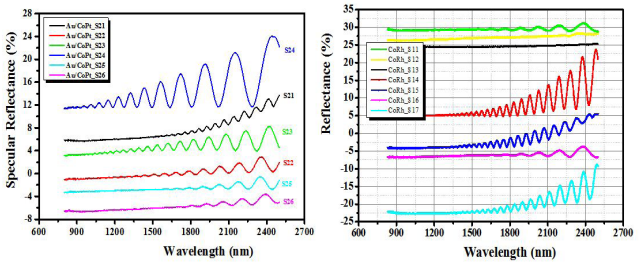


**Figure 9:** Total reflection spectra of our two series (CoPt and CoRh) of samples as electrodeposited.

As far as we know, this reflectance oscillation could be also due to the oscillatory exchange coupling across the nonmagnetic layers M in Cobalt layers as function of thickness of M layers. It follows that the oscillations in these systems are approximately periodic, and the period change with the change of thickness. This phenomena has been discovered by Parkin et al., [1]. Therefore, it is expected that the cylindrical shape of the nanowires has a significant influence on their optical properties.

## Conclusion

Multilayered Co/M thin films nanowires having a face centered cubic and a hexagonal compact mixed lattices were successfully fabricated by electrochemical deposition in ion track-etched polycarbonate templates. From X-ray diffraction characterization the wires exhibit a strong (10.1) texture. The SEM and AFM images displayed the morphology and revealed that the wires have excellent cylindrical

shape, smooth and homogeneous contours along their long axis. MFM image shows that the magnetization is perpendicular to the wires axis in conformity to the result found for the Co wires. The polarity alternation suggests the reversal of magnetization in the perpendicular plane in function of wires' length. From the optical spectra, the multilayered thin films NWs show a broad reflectance band from ≈900nm to ≈2500nm which is ascribed to a surface plasmon-resonance and the thin films behavior. The magnetization reversal strongly depends on the variation of the aspect ratio (thickness/diameter) between cobalt and M (M=Pt, or Rh) layers. Therefore, the change of the thickness (wires length) or the pores diameter (wide) was seen to control the properties of the multilayered thin films NWs and hence their properties could be modified for desired purpose. Hence one can say that the multilayered Co/M thin films NWs stack with many layers can be a good candidate for electro-optic, telecommunications, solar concentrator and architectural applications.

## Acknowledgement

This work was supported financially by TWAS-UNESCO Associateship Scheme under the Research Project - Ref. 3240290071.

One of the authors (Prof. Dr A. Kazadi Mukenga Bantu) would like to express his appreciation and thanks to Prof. M. Maaza Nanosciences African network (NANOAFNET), Materials Research Department (MRD), iThemba LABS-National Research Foundation (NRF), Somerset West, South Africa for his valuable suggestions, fruitful discussion, availability, constant support, help and encouragement. Also very heartfelt thanks to all the staff members of the Materials Research Group (MRG-iThemba Labs) for giving me the opportunity, time and facilities to complete this work.

## References

1. Parkin SS, More N, Roche KP (1990) Oscillations in exchange coupling and magnetoresistance in metallic superlattice structures: Co/Ru, Co/Cr, and Fe/Cr. Phys Rev Lett 64: 2304-2307.

2. Bruno P, Chappert C (1991) Oscillatory coupling between ferromagnetic layers separated by a nonmagnetic metal spacer. Phys Rev Lett 67: 1602-1605.

3. Fert AR (1991) Magnetic and Transport Properties of Metallic Multilayers. Materials Science Forum 59: 439-480.

4. Kuchibhatla SVNT, Karakoti AS, Bera D, Seal S (2007) One dimensional nanostructured materials. Prog Mater Sci 52: 699-913.

5. Ross CA (2001) Patterned Magnetic Recording Media. Annu Rev Mater Res 31: 203-235.

6. Vila L, Vincent P, Pra LDD, Pirio G, Minoux E, et al. (2004) Growth and Field-Emission Properties of Vertically Aligned Cobalt Nanowire Arrays. Nano Lett 4: 521-524.

7. Xavier S, Mátéfi-Tempfli S, Ferain E, Purcell S, Enouz-Védrenne S, et al. (2008) Stable field emission from arrays of vertically aligned free-standing metallic nanowires. Nanotechnology 19: 215601.

8. Huang X, Li L, Luo X, Zhu X, Li G (2008) Orientation-Controlled Synthesis and Ferromagnetism of Single Crystalline Co Nanowire Arrays. J Phys Chem C 112: 1468-1472.

9. Niu H, Chen Q, Zhu H, Lin Y, Zhang X (2003) Magnetic field-induced growth and self-assembly of cobalt nanocrystallites . J Mater Chem 13: 1803-1805.

10. Thurn-Albrecht T, Schotter J, Kästle GA, Emley N, Shibauchi T, et al. (2000) Ultrahigh-density nanowire arrays grown in self-assembled diblock copolymer templates. Science 290: 2126-2129.

11. Liu J, Duan JL, Toimil-Molares ME, Karim S, Cornelius TW, et al. (2006) Electrochemical fabrication of single-crystalline and polycrystalline Au nanowires: the influence of deposition parameters. Nanotechnology 17: 1922.

12. Whitney TM, Jiang JS, Searson PC, Chien CL (1993) Fabrication and Magnetic Properties of Arrays of Metallic Nanowires. Science 261: 1316-1319.

13. Piraux L, George JM, Despres JF, Leroy C, Ferain E, et al. (1994) Giant magnetoresistance in magnetic multilayered nanowires. Appl Phys Lett 65: 484-486.

14. Blondel A, Meier JP, Doudin B, Ansermet JP (1994) Giant magnetoresistance of nanowires of multilayers. Appl Phys Lett 65: 3019-3021.

15. Cornelius TW, Brötz J, Chtanko N, Dobrev D, Miehe G, et al. (2005) Controlled fabrication of poly- and single-crystalline bismuth nanowires. Nanotechnology 16: 246.

16. Bantu AKM, Rivas J, Zaragoza G, López-Quintela MA, Blanco MC (2001) Structure and magnetic properties of electrodeposited cobalt nanowires. J Appl Phys 89: 3393-3397.

17. Maurer F, Brötz J, Karim S, Toimil Molares ME, Trautmann C, et al. (2007) Preferred growth orientation of metallic fcc nanowires under direct and alternating electrodeposition conditions. Nanotechnology 18: 135709.

18. Ni X, Ma J, Li J, Huang J, Jiao D, et al. (2008) Structure and microwave characteristics of Co/TiO2 nanocomposites prepared by ball milling. J Nanosci Nanotechnol 8: 4470-4476.

19. Huang JY, Wu YK, Ye HQ (1996) Deformation structures in ball milled copper. Acta Mater 44: 1211-1221.

20. Nakahara S, Mahajan S (1980) The Influence of Solution pH on Microstructure of Electrodeposited Cobalt. J Electrochem Soc 127: 283-288.

21. Bantu AKM, Castro ACDE, Magalhaes SDDE, Barthem VMTS, Givord D, et al. (2014) Structural and Magnetic Properties of Electrodeposited CoPt and FeCu Nanowires Embedded in Polycarbonate Membranes. The African Review of Physics **9:** 487-496.

22. Duan J, Liu J, Yao H, Mo D, Hou M, et al. (2008) Sci Eng 57.

23. Kreibig U, Vollmer M (1995) Optical Properties of Metal Clusters. Springer 25: 532.


Journal of Anesthesia & Clinical Care

Journal of Addiction & Addictive Disorders

Advances in Microbiology Research

Advances in Industrial Biotechnology

Journal of Agronomy & Agricultural Science

Journal of AIDS Clinical Research & STDs

Journal of Alcoholism, Drug Abuse & Substance Dependence

Journal of Allergy Disorders & Therapy

Journal of Alternative, Complementary & Integrative Medicine

Journal of Alzheimer's & Neurodegenerative Diseases

Journal of Angiology & Vascular Surgery

Journal of Animal Research & Veterinary Science

Archives of Zoological Studies

Archives of Urology

Journal of Atmospheric & Earth-Sciences

Journal of Aquaculture & Fisheries

Journal of Biotech Research & Biochemistry

Journal of Brain & Neuroscience Research

Journal of Cancer Biology & Treatment

Journal of Cardiology: Study & Research

Journal of Cell Biology & Cell Metabolism

Journal of Clinical Dermatology & Therapy

Journal of Clinical Immunology & Immunotherapy

Journal of Clinical Studies & Medical Case Reports

Journal of Community Medicine & Public Health Care

Current Trends: Medical & Biological Engineering

Journal of Cytology & Tissue Biology

Journal of Dentistry: Oral Health & Cosmesis

Journal of Diabetes & Metabolic Disorders

Journal of Dairy Research & Technology

Journal of Emergency Medicine Trauma & Surgical Care

Journal of Environmental Science: Current Research

Journal of Food Science & Nutrition

Journal of Forensic, Legal & Investigative Sciences

Journal of Gastroenterology & Hepatology Research

Journal of Gerontology & Geriatric Medicine

Journal of Genetics & Genomic Sciences

Journal of Hematology, Blood Transfusion & Disorders

Journal of Human Endocrinology

Journal of Hospice & Palliative Medical Care

Journal of Internal Medicine & Primary Healthcare

Journal of Infectious & Non Infectious Diseases

Journal of Light & Laser: Current Trends

Journal of Modern Chemical Sciences

Journal of Medicine: Study & Research

Journal of Nanotechnology: Nanomedicine & Nanobiotechnology

Journal of Neonatology & Clinical Pediatrics

Journal of Nephrology & Renal Therapy

Journal of Non Invasive Vascular Investigation

Journal of Nuclear Medicine, Radiology & Radiation Therapy

Journal of Obesity & Weight Loss

Journal of Orthopedic Research & Physiotherapy

Journal of Otolaryngology, Head & Neck Surgery

Journal of Protein Research & Bioinformatics

Journal of Pathology Clinical & Medical Research

Journal of Pharmacology, Pharmaceutics & Pharmacovigilance

Journal of Physical Medicine, Rehabilitation & Disabilities

Journal of Plant Science: Current Research

Journal of Psychiatry, Depression & Anxiety

Journal of Pulmonary Medicine & Respiratory Research

Journal of Practical & Professional Nursing

Journal of Reproductive Medicine, Gynaecology & Obstetrics

Journal of Stem Cells Research, Development & Therapy

Journal of Surgery: Current Trends & Innovations

Journal of Toxicology: Current Research

Journal of Translational Science and Research

Trends in Anatomy & Physiology

Journal of Vaccines Research & Vaccination

Journal of Virology & Antivirals

Archives of Surgery and Surgical Education

Sports Medicine and Injury Care Journal

International Journal of Case Reports and Therapeutic Studies

Journal of Ecology Research and Conservation Biology

Submit Your Manuscript: http://www.heraldopenaccess.us/Online-Submission.php

Herald Scholarly Open Access, 2561 Cornelia Rd, #205, Herndon, VA 20171, USA.
Tel: +1 202-499-9679; E-mail: info@heraldsopenaccess.us
http://www.heraldopenaccess.us/